

Hydrothermal Syntheses and Single-Crystal Structures of Some Novel Guanidinium–Zinc–Phosphates

William T. A. Harrison*

Department of Chemistry, University of Western Australia, Nedlands, WA 6907, Australia

Mark L. F. Phillips†

Sandia National Laboratories, Albuquerque, New Mexico 87185

Received March 3, 1997. Revised Manuscript Received May 12, 1997[⊗]

The mild-condition hydrothermal syntheses and single-crystal structures of three new guanidinium zinc phosphates are reported. $\text{CN}_3\text{H}_6\cdot\text{Zn}_2(\text{HPO}_4)_2\text{H}_2\text{PO}_4$ and $(\text{CN}_3\text{H}_6)_2\cdot\text{Zn}(\text{HPO}_4)_2$ are built up from three-dimensional Zn/P/O frameworks encapsulating guanidinium cations in 12-ring channel systems. The latter material has the lowest nodal-framework-atom density per unit volume of any open-framework phase characterized so far. $(\text{CN}_3\text{H}_6)_6\cdot\text{Zn}_2(\text{OH})(\text{PO}_4)_3\cdot\text{H}_2\text{O}$ is a one-dimensional phase with respect to Zn/P/O connectivity and has a unique triply bridged tetrahedral chain connectivity for simple phosphates. Crystal data: $\text{CN}_3\text{H}_6\cdot\text{Zn}_2(\text{HPO}_4)_2\text{H}_2\text{PO}_4$, $M_r = 478.78$, monoclinic, space group $P2_1$ (No. 4), $a = 5.1318(4)$ Å, $b = 7.8411(7)$ Å, $c = 16.510(1)$ Å, $\beta = 90.110(7)^\circ$, $V = 664.36(8)$ Å³, $Z = 2$, $R = 2.43\%$, $R_w = 2.67\%$ [2608 observed reflections with $I > 3\sigma(I)$]. $(\text{CN}_3\text{H}_6)_2\cdot\text{Zn}(\text{HPO}_4)_2$, $M_r = 377.50$, orthorhombic, space group $Pna2_1$ (No. 33), $a = 10.447(2)$ Å, $b = 12.349(2)$ Å, $c = 10.225(2)$ Å, $V = 1319.2(5)$ Å³, $Z = 4$, $R = 3.26\%$, $R_w = 3.32\%$ [2252 observed reflections with $I > 3\sigma(I)$]. $(\text{CN}_3\text{H}_6)_6\cdot\text{Zn}_2(\text{OH})(\text{PO}_4)_3\cdot\text{H}_2\text{O}$, $M_r = 811.17$, trigonal, space group $R\bar{3}$ (No. 148), $a = 20.016(7)$ Å, $c = 13.955(6)$ Å, $V = 4842(4)$ Å³, $Z = 6$, $R = 5.31\%$, $R_w = 5.52\%$ [630 observed reflections with $I > 3\sigma(I)$].

Introduction

Over the past few years, it has become apparent that non-aluminosilicate open-framework phases—inorganic materials that contain voids and channels of appreciable size occupied by “guest” species—have an astonishingly diverse structural chemistry.^{1–8} Our own work, largely focused on the tetrahedral-building-unit zincophosphate/arsenate (ZnPO/ZnAsO) system, has revealed direct analogues of aluminosilicate zeolites,⁹ complex organically templated networks,¹⁰ and a family of robust, thermally stable phases based on a completely new type of topology involving ZnO_4 , PO_4 , and novel OZn_4 tetrahedral units.¹¹

One persistent problem in this area of materials chemistry is a fundamental lack of control in directing a reaction toward a desired framework configuration. A major reason for this difficulty is that in general, the mechanisms of mild-condition kinetically controlled reactions are poorly understood.¹² Predictive crystal packing models based on “common sense” or symmetry arguments¹³ are of little assistance in this field. Following the methodology of classical aluminosilicate zeolite preparations,¹⁴ exploratory synthesis retains a vital role in this area at present. An especially important concept involves *templating*—the tendency of a particular component of the reaction, usually a cation, to direct the reaction to a particular structure, or at least a structure containing a distinct feature. A simple example for non-aluminosilicate materials appears to be the predilection for Li^+ to template tetrahedral 6-rings in beryllophosphate networks,¹⁵ based on size considerations in terms of optimizing Li–O tetrahedral bond lengths. Small organic molecules, particularly those containing amino groups, have played an outstanding role in templating novel networks.^{16,17} In some cases there is a striking and beautiful relationship between the template shape and the surrounding framework topology.¹⁸

* Present address: Deacon Research, 2440 Embarcadero Way, Palo Alto, CA 94303.

† Abstract published in *Advance ACS Abstracts*, July 1, 1997.

(1) Haushalter, R. C.; Mundi, L. A. *Chem. Mater.* **1992**, *4*, 31 and included references.

(2) Estermann, M.; McCusker, L. B.; Baerlocher, Ch.; Merrouche, A.; Kessler, H. *Nature (London)* **1991**, *352*, 320.

(3) Loiseau, T.; Férey, G. *J. Solid State Chem.* **1994**, *111*, 416.

(4) Chen, J.; Jones, R. H.; Natarajan, S.; Hursthouse, M. B.; Thomas, J. M. *Angew. Chem., Int. Ed. Engl.* **1994**, *33*, 639.

(5) Chippindale, A. M.; Walton, R. I. *J. Chem. Soc., Chem. Commun.* **1994**, 2453.

(6) Song, T.; Hursthouse, M. B.; Chen, J.; Xu, J.; Malik, K. M. A.; Jones, R. H.; Xu, R.; Thomas, J. M. *Adv. Mater.* **1994**, *6*, 679.

(7) Natarajan, S.; Gabriel, J.-C. P.; Cheetham, A. K. *J. Chem. Soc., Chem. Commun.* **1996**, 1415.

(8) Khan, M. I.; Meyer, L. M.; Haushalter, R. C.; Schweizer, A. L.; Zubieta, J.; Dye, J. L. *Chem. Mater.* **1996**, *8*, 43 and included references.

(9) Gier T. E.; Stucky, G. D. *Nature (London)* **1991**, *349*, 508.

(10) Harrison, W. T. A.; Gier, T. E.; Martin, T. E.; Stucky, G. D. *J. Mater. Chem.* **1992**, *2*, 175. Feng, P.; Bu, X.; Stucky, G. D. *Angew. Chem., Int. Ed. Engl.* **1995**, *34*, 1745. Bu, X.; Feng, P.; Stucky, G. D. *J. Solid State Chem.* **1996**, *125*, 243.

(11) Harrison, W. T. A.; Broach, R. W.; Bedard, R. A.; Gier, T. E.; Bu, X.; Stucky, G. D. *Chem. Mater.* **1996**, *8*, 691.

(12) Davis, M. E.; Lobo, R. F. *Chem. Mater.* **1992**, *4*, 756.

(13) Brock, C. P.; Dunitz, J. D. *Chem. Mater.* **1994**, *6*, 1118.

(14) Breck, D. W. *Zeolite Molecular Sieves*; Wiley: New York, 1974.

(15) Harrison, W. T. A.; Gier, T. E.; Stucky, G. D. *Zeolites* **1993**, *13*, 242.

(16) Flanigen, E. M.; Lok, B. M.; Patton, R. L.; Wilson, S. T. In *New Developments in Zeolite Science and Technology*; Elsevier: Amsterdam, 1986; p 103.

(17) Bonavia, G.; Haushalter, R. C.; O'Connor, C. J.; Zubieta, J. *Inorg. Chem.* **1996**, *35*, 5603.

Table 1. Synthesis Schemes

| compound | prepared from: | | | | ratio ^a | product |
|---|--|--------------------------------|------------------|--------------------|--------------------|---------------------------------|
| | (C(NH ₂) ₃) ₂ CO ₃ | H ₃ PO ₄ | H ₂ O | ZnO | | |
| CN ₃ H ₆ ·Zn ₂ (HPO ₄) ₂ H ₂ PO ₄ | 1.20 g (0.0067 mol) | 3.83 g (0.033 mol) | 9.32 g | 0.814 g (0.01 mol) | 4:3:10 | transparent blocks/white powder |
| (CN ₃ H ₆) ₂ ·Zn(HPO ₄) ₂ | 0.72 g (0.004 mol) | 1.38 g (0.012 mol) | 10.28 g | 0.814 g (0.01 mol) | 4:5:6 | jagged lumps/white powder |
| (CN ₃ H ₆) ₆ ·Zn ₂ (OH)(PO ₄) ₃ ·H ₂ O | 5.40 g (0.03 mol) | 2.29 g (0.02 mol) | 9.92 g | 0.814 g (0.01 mol) | 6:1:2 | small rods/white powder |

^a Starting ratio of guanidine:zinc:phosphorus.

Table 2. Crystallographic Parameters

| | CN ₃ H ₆ ·Zn ₂ (HPO ₄) ₂ H ₂ PO ₄ | (CN ₃ H ₆) ₂ ·Zn(HPO ₄) ₂ | (CN ₃ H ₆) ₆ ·Zn ₂ (OH)(PO ₄) ₃ ·H ₂ O |
|--|---|---|---|
| emp formula | Zn ₂ P ₃ O ₁₂ N ₃ C ₁ H ₉ | Zn ₁ P ₂ O ₈ N ₆ C ₂ H ₁₄ | Zn ₂ P ₃ O ₁₄ N ₁₈ C ₆ H ₃₉ |
| formula wt | 478.78 | 377.50 | 811.17 |
| crystal system | Monoclinic | Orthorhombic | Trigonal |
| <i>a</i> (Å) | 5.1318 (4) | 10.447 (2) | 20.016 (7) |
| <i>b</i> (Å) | 7.8411 (7) | 12.349 (2) | 20.016 (7) |
| <i>c</i> (Å) | 16.510 (1) | 10.225 (2) | 13.955 (6) |
| α (deg) | 90 | 90 | 90 |
| β (deg) | 90.119 (7) | 90 | 90 |
| γ (deg) | 90 | 90 | 120 |
| <i>V</i> (Å ³) | 664.36 (8) | 1319.2 (5) | 4842 (4) |
| <i>Z</i> | 2 | 4 | 6 |
| space group | <i>P</i> 2 ₁ (No. 4) | <i>P</i> na2 ₁ (No. 33) | <i>R</i> $\bar{3}$ (No. 148) |
| <i>T</i> (°C) | 25 (2) | 25 (2) | 25 (2) |
| λ (Mo Kα) (Å) | 0.71073 | 0.71073 | 0.71073 |
| ρ _{calc} (g/cm ³) | 2.39 | 1.90 | 1.67 |
| μ (cm ⁻¹) | 41.2 | 21.9 | 17.5 |
| total data | 3639 | 3475 | 1329 |
| obsd data ^a | 2608 | 2252 | 630 |
| parameters | 211 | 179 | 137 |
| <i>R</i> (F) ^b | 2.43 | 3.26 | 5.31 |
| <i>R</i> _w (F) ^c | 2.67 | 3.32 | 5.52 |

^a $I > 3\sigma(I)$ after data merging. ^b $R = 100\sum||F_o| - |F_c||/\sum|F_o|$. ^c $R_w = 100[\sum w(|F_o| - |F_c|)^2/\sum w|F_o|^2]^{1/2}$.

An interesting candidate for templating inorganic frameworks that has not received much attention so far is the nitrogen-rich guanidinium cation [C(NH₂)₃⁺ or CN₃H₆⁺]. The assumption of delocalization of its positive charge over its three "arms" and the resulting symmetrical, rigid "propeller" shape of this cation¹⁹ suggested to us that in a designer synthesis,²⁰ this species might act to template medium-sized rings in side-on orientation (i.e., the C and N atoms of the guanidinium cation are approximately aligned in the plane of the ring), with the involvement of N–H···O hydrogen bonds to framework oxygen atoms. The guanidinium cation is known to show a similar mode of bonding in adopting a side-on orientation when occupying molecular crown ether rings.²¹

In this paper, we describe our investigations into zincophosphate networks templated by the guanidinium cation. Three new phases have been prepared as single crystals by variations on a simple solution-phase reaction. (CN₃H₆)₂·Zn(HPO₄)₂ and CN₃H₆·Zn₂(HPO₄)₂H₂PO₄ are three-dimensional open-framework structures incorporating extraframework guanidinium cations, whereas (CN₃H₆)₆·Zn₂(OH)(PO₄)₃·H₂O is one-dimensional (or "polymeric") with respect to Zn/P/O connectivity and contains a triply bridged tetrahedral chain structure which is unprecedented for simple phosphate materials.

Experimental Section

Synthesis and Initial Characterization. The three title compounds were prepared from guanidinium carbonate [(C(NH₂)₃)₂CO₃, Kodak], phosphoric acid (85% H₃PO₄, Fisher) deionized water and zinc oxide (ZnO, St. Joseph's), as shown in Table 1. In each case, the ZnO was added to an aqueous solution of (C(NH₂)₃)₂CO₃ and H₃PO₄, and the resulting mixture was shaken well and aged for 1 day at room temperature. The mixture, enclosed in a 100 mL PTFE bottle, was then placed in a 100 °C oven for 5 days. The solid product was recovered from the supernatant liquors by filtration.

X-ray powder diffraction data (Siemens D500 automated diffractometer, Cu Kα radiation, λ = 1.5418 Å) were recorded for crushed crystals of each phase and revealed complex patterns, unlike those of the starting materials or known zinc phosphates.

Single-Crystal Structure Determinations. In each case, a suitable crystal (for CN₃H₆·Zn₂(HPO₄)₂H₂PO₄, transparent block, dimensions ~0.4 × 0.2 × 0.2 mm; for (CN₃H₆)₂·Zn(HPO₄)₂, irregular "glassy" chunk, ~0.6 × 0.5 × 0.5 mm; for (CN₃H₆)₆·Zn₂(OH)(PO₄)₃·H₂O, translucent rod, ~0.4 × 0.15 × 0.15 mm) was selected and glued to a thin glass fiber with cyanoacrylate adhesive and mounted on a Siemens P4 automated diffractometer (graphite monochromated Mo Kα radiation, λ = 0.710 73 Å). Room temperature [25(2) °C] data collections were performed after the unit cells were established and optimized by the standard procedures of peak-search, centering, indexing, and least-squares routines. Refined cell parameters for CN₃H₆·Zn₂(HPO₄)₂H₂PO₄ (monoclinic), (CN₃H₆)₂·Zn(HPO₄)₂ (orthorhombic), and (CN₃H₆)₆·Zn₂(OH)(PO₄)₃·H₂O (trigonal–rhombohedral) are presented in Table 2. The unit cell of CN₃H₆·Zn₂(HPO₄)₂H₂PO₄ was carefully optimized using high-angle reflections to accurately determine the monoclinic β angle. Monoclinic symmetry was confirmed by scanning (would-be) equivalent reflections to check their intensity consistencies in 2/*m* (monoclinic) and *mmm* (orthorhombic) Laue symmetry.

(18) Lawton, S. L.; Rohrbaugh, *Science (Washington, D.C.)* **1990**, *247*, 1319.

(19) Lyxell, D.-G.; Strandberg, R. *Acta Crystallogr.* **1988**, *C44*, 1535.

(20) Harrison, W. T. A.; Phillips, M. L. F. *Chem. Commun.* **1996**, 2781.

(21) Uiterwijk, J. W. H. M.; Harkema, S.; Geevers, J.; Reinhoudt, D. N. *J. Chem. Soc., Chem. Commun.* **1982**, 200.

Data were collected using the $\omega/2\theta$ scan mode to a maximum 2θ of 65° for $\text{CN}_3\text{H}_6\cdot\text{Zn}_2(\text{HPO}_4)_2\text{H}_2\text{PO}_4$ and $(\text{CN}_3\text{H}_6)_2\cdot\text{Zn}(\text{HPO}_4)_2$. The $(\text{CN}_3\text{H}_6)_6\cdot\text{Zn}_2(\text{OH})(\text{PO}_4)_3\cdot\text{H}_2\text{O}$ crystal was a very weak scatterer, and data were collected to a maximum 2θ of 40° for this material. Intensity standards, remeasured every 100 observations, showed only statistical fluctuations over the course of the three data collections. Absorption was monitored by ψ scans and corrected for at the data reduction stage²² (ranges of equivalent transmission factors: $\text{CN}_3\text{H}_6\cdot\text{Zn}_2(\text{HPO}_4)_2\text{H}_2\text{PO}_4$: 0.57–0.63; $(\text{CN}_3\text{H}_6)_2\cdot\text{Zn}(\text{HPO}_4)_2$: 0.55–0.57; $(\text{CN}_3\text{H}_6)_6\cdot\text{Zn}_2(\text{OH})(\text{PO}_4)_3\cdot\text{H}_2\text{O}$: 0.88–0.99). The raw intensities were reduced to F and $\sigma(F)$ values by means of a profile-fitting routine,²³ the normal corrections for Lorentz and polarization factors were made, and the equivalent data merged, applying the observability criterion $I > 3\sigma(I)$: for $\text{CN}_3\text{H}_6\cdot\text{Zn}_2(\text{HPO}_4)_2\text{H}_2\text{PO}_4$, 3639 reflections merged to 2608 observed reflections with $R_{\text{int}} = 0.032$; for $(\text{CN}_3\text{H}_6)_2\cdot\text{Zn}(\text{HPO}_4)_2$, 3475 reflections merged to 2252 observed reflections with $R_{\text{int}} = 0.030$; for $(\text{CN}_3\text{H}_6)_6\cdot\text{Zn}_2(\text{OH})(\text{PO}_4)_3\cdot\text{H}_2\text{O}$, 1329 reflections merged to 630 observed reflections with $R_{\text{int}} = 0.079$.

For $\text{CN}_3\text{H}_6\cdot\text{Zn}_2(\text{HPO}_4)_2\text{H}_2\text{PO}_4$, the systematic absences in the reduced data ($0k0$, $k \neq 2n$) indicated space groups $P2_1$ or $P2_1/m$. For $(\text{CN}_3\text{H}_6)_2\cdot\text{Zn}(\text{HPO}_4)_2$, the absence conditions $0kl$, $k + l \neq 2n$; $h0l$, $h \neq 2n$; and $00l$, $l \neq 2n$, indicated space groups $Pna2_1$ or $Pnam$. For $(\text{CN}_3\text{H}_6)_6\cdot\text{Zn}_2(\text{OH})(\text{PO}_4)_3\cdot\text{H}_2\text{O}$, the systematic absences $h\bar{h}0l$, $h + l \neq 3n$ and $000l$, $l \neq 3n$ indicated space groups $R\bar{3}$, $R\bar{3}$, $R\bar{3}2$, $R\bar{3}m$, or $R\bar{3}m$. Trial reflection merges indicated that Laue class $\bar{3}$, as opposed to $\bar{3}m$, was probably applicable to this phase.

The structures of these phases were solved by direct methods using SHELXS86.²⁴ In each case, a sufficient fragment of the structure was revealed (Zn, P, some O) to enable the remainder of the non-hydrogen atoms to be located from Fourier difference maps, and the refinements to proceed straightforwardly to the $R < 10\%$ stage (isotropic thermal parameters). For $\text{CN}_3\text{H}_6\cdot\text{Zn}_2(\text{HPO}_4)_2\text{H}_2\text{PO}_4$ and $(\text{CN}_3\text{H}_6)_2\cdot\text{Zn}(\text{HPO}_4)_2$, only the noncentrosymmetric space groups [$P2_1$ (No. 4) and $Pna2_1$ (No. 33), respectively] revealed a reasonable starting configuration. For $(\text{CN}_3\text{H}_6)_6\cdot\text{Zn}_2(\text{OH})(\text{PO}_4)_3\cdot\text{H}_2\text{O}$, the best model was established in the centrosymmetric space group $R\bar{3}$ (No. 148). In each refinement, a Larson-type secondary extinction correction²⁵ was optimized at the latter stages of the refinement to improve the fit of strong, low-angle reflections which showed a systematic $F_{\text{obs}} < F_{\text{calc}}$ trend. Full-matrix least-squares refinements and all subsidiary calculations were performed with the Oxford CRYSTALS²⁶ system.

For $\text{CN}_3\text{H}_6\cdot\text{Zn}_2(\text{HPO}_4)_2\text{H}_2\text{PO}_4$, several difference-map features corresponding to probable "framework" proton sites were located. The resulting H atom positions were refined using O–H and N–H bond length and P–O–H and C–N–H bond angle restraints to ensure a stable refinement. Hydrogen atoms associated with the guanidinium cation were located geometrically by assuming planar sp^2 hybridization about each N atom and an N–H bond length of 0.95 Å. The Flack polarity parameter²⁷ was optimized to establish the absolute structure of the individual crystal of $\text{CN}_3\text{H}_6\cdot\text{Zn}_2(\text{HPO}_4)_2\text{H}_2\text{PO}_4$ studied in the diffraction experiment. A refined value of 0.00(2) indicated that the absolute structure is as given in the Results. Final residuals of $R = 2.43\%$ and $R_w = 2.67\%$ ($w_i = 1/\sigma^2$) were obtained for refinements varying positional and anisotropic thermal parameters for all non-hydrogen atoms and an atom-type isotropic thermal factor for H. Setting the Flack parameter to 1.00 (opposite absolute structure) and repeating the refinement resulted in residuals of $R = 3.34\%$ and $R_w = 3.89\%$. Because no chiral reagents were used in the synthesis, there is no reason to suspect that the bulk sample of $\text{CN}_3\text{H}_6\cdot$

Table 3. Final Atomic Coordinates/Thermal Factors for $\text{CN}_3\text{H}_6\cdot\text{Zn}_2(\text{HPO}_4)_2\text{H}_2\text{PO}_4$

| atom | <i>x</i> | <i>y</i> | <i>z</i> | U_{eq}^a |
|-------|------------|------------|------------|-------------------|
| Zn(1) | 0.19821(8) | 0.1421(1) | 0.58625(2) | 0.0131 |
| Zn(2) | 0.19570(8) | 0.3706(1) | 0.92089(2) | 0.0137 |
| P(1) | −0.2965(2) | 0.2656(2) | 0.49857(5) | 0.0121 |
| P(2) | 0.3056(2) | 0.7555(2) | 0.98746(5) | 0.0124 |
| P(3) | 0.4539(2) | 0.2507(2) | 0.75346(5) | 0.0157 |
| O(1) | −0.1497(5) | 0.2392(4) | 0.5785(1) | 0.0161 |
| O(2) | 0.3285(5) | 0.1284(5) | 0.6950(2) | 0.0217 |
| O(3) | 0.1885(5) | −0.0917(4) | 0.5515(2) | 0.0183 |
| O(4) | 0.4131(5) | 0.2896(4) | 0.5166(2) | 0.0168 |
| O(5) | 0.1951(5) | 0.6122(4) | 0.9369(2) | 0.0192 |
| O(6) | −0.1563(5) | 0.2855(4) | 0.9339(2) | 0.0184 |
| O(7) | 0.4065(5) | 0.2263(4) | 0.9915(2) | 0.0181 |
| O(8) | 0.2751(5) | 0.3486(5) | 0.8079(2) | 0.0227 |
| O(9) | −0.2550(6) | 0.1035(4) | 0.4436(2) | 0.0198 |
| O(10) | 0.2773(7) | 0.9160(4) | 0.9319(2) | 0.0236 |
| O(11) | 0.6143(6) | 0.3889(5) | 0.7067(2) | 0.0270 |
| O(12) | 0.6460(6) | 0.1375(5) | 0.8040(2) | 0.0233 |
| C(1) | −0.1181(8) | −0.2448(7) | 0.7414(2) | 0.0246 |
| N(1) | −0.2211(8) | −0.2397(7) | 0.8157(2) | 0.0327 |
| N(2) | 0.0985(8) | −0.3280(6) | 0.7274(2) | 0.0323 |
| N(3) | −0.2394(8) | −0.1643(6) | 0.6815(2) | 0.0313 |

$$^a U_{\text{eq}} (\text{\AA}^2) = 1/3[U_1 + U_2 + U_3].$$

$\text{Zn}_2(\text{HPO}_4)_2\text{H}_2\text{PO}_4$ consists of anything other than a random 50:50 mixture of crystals of both absolute structures.

For $(\text{CN}_3\text{H}_6)_2\cdot\text{Zn}(\text{HPO}_4)_2$, the refinement proceeded straightforwardly in space group $Pna2_1$. Guanidinium-cation hydrogen atoms were located geometrically, as above. Refinement of the Flack parameter to ~ 1.0 indicated that the incorrect absolute structure had been established in the initial model. The polarity of the model was reversed by changing the sign of the polar-axis z coordinate for all the atoms and re-refining the model, which resulted in a final value for the Flack parameter of $-0.01(2)$ and residuals of $R = 3.26\%$ and $R_w = 3.32\%$ ($w_i = 1/\sigma^2$). Re-refinement of this transformed coordinate set with the Flack parameter set to 1.00 led to residuals of $R = 4.17\%$ and $R_w = 4.50\%$. Once again, we assume the bulk sample of $(\text{CN}_3\text{H}_6)_2\cdot\text{Zn}(\text{HPO}_4)_2$ contains 50% of each absolute structure.

For $(\text{CN}_3\text{H}_6)_6\cdot\text{Zn}_2(\text{OH})(\text{PO}_4)_3\cdot\text{H}_2\text{O}$ no proton positions could be located in difference maps. Guanidinium cation hydrogen atoms were located geometrically, as above. Anisotropic thermal parameter refinement of the bridging Zn–O–Zn oxygen atoms O(5) and O(6) (vide infra) resulted in "pancaked" thermal ellipsoids perpendicular to [0001] which converged to nonpositive-definite values. These were reset to isotropic for the final refinement cycles, which resulted in final residuals of $R = 5.31\%$ and $R_w = 5.52\%$ ($w_i = 1/\sigma^2$).

Results

Crystal Structure of $\text{CN}_3\text{H}_6\cdot\text{Zn}_2(\text{HPO}_4)_2\text{H}_2\text{PO}_4$

This material forms a new anionic open-framework phase built up from tetrahedral ZnO_4 and PO_4 building blocks, connected via Zn–O–P bonds, surrounding channels occupied by extraframework guanidinium cations. Final atomic coordinates and thermal parameters for $\text{CN}_3\text{H}_6\cdot\text{Zn}_2(\text{HPO}_4)_2\text{H}_2\text{PO}_4$ are presented in Table 3, with selected geometrical data in Table 4. The building unit of $\text{CN}_3\text{H}_6\cdot\text{Zn}_2(\text{HPO}_4)_2\text{H}_2\text{PO}_4$ is shown in Figure 1 using CAMERON,²⁸ and the complete crystal structure is illustrated in Figure 2.

The two zinc atoms in $\text{CN}_3\text{H}_6\cdot\text{Zn}_2(\text{HPO}_4)_2\text{H}_2\text{PO}_4$ are both tetrahedrally coordinated by their O atom neighbors with average zinc–oxygen bond distances of 1.939(2) Å for Zn(1) and 1.930(2) Å for Zn(2). Both zinc atoms make four Zn–O–P bonds to four distinct P-atom

(22) XSCANS Program Suite, Siemens Inc., Madison, WI.

(23) Lehman, M. S.; Larsen, F. K. *Acta Crystallogr.* **1974**, *A30*, 580.

(24) Sheldrick, G. M. SHELXS86 User Guide, University of Göttingen, Germany.

(25) Larson, A. C. *Acta Crystallogr.* **1967**, *23*, 664.

(26) Watkin, D. J.; Carruthers, J. R.; Betteridge, P. W. CRYSTALS User Guide, Chemical Crystallography Laboratory, University of Oxford, UK.

(27) Flack, H. D. *Acta Crystallogr.* **1983**, *A39*, 876.

(28) Pearce, L. M.; Prout, C. K.; Watkin, D. J. CAMERON user guide, Chemical Crystallography Laboratory, University of Oxford, UK.

Table 4. Selected Bond Distances (Å) and Angles (deg) for $\text{CN}_3\text{H}_6 \cdot \text{Zn}_2(\text{HPO}_4)_2\text{H}_2\text{PO}_4$

| | | | |
|-----------------|----------|------------------|----------|
| Zn(1)–O(1) | 1.945(3) | Zn(1)–O(2) | 1.918(3) |
| Zn(1)–O(3) | 1.922(3) | Zn(1)–O(4) | 1.970(3) |
| Zn(2)–O(5) | 1.913(3) | Zn(2)–O(6) | 1.938(3) |
| Zn(2)–O(7) | 1.950(3) | Zn(2)–O(8) | 1.919(3) |
| P(1)–O(1) | 1.532(3) | P(1)–O(3) | 1.498(3) |
| P(1)–O(4) | 1.532(2) | P(1)–O(9) | 1.576(3) |
| P(2)–O(5) | 1.510(3) | P(2)–O(6) | 1.527(3) |
| P(2)–O(7) | 1.534(3) | P(2)–O(10) | 1.564(3) |
| P(3)–O(2) | 1.503(3) | P(3)–O(8) | 1.497(3) |
| P(3)–O(11) | 1.566(3) | P(3)–O(12) | 1.566(3) |
| C(1)–N(1) | 1.337(5) | C(1)–N(2) | 1.310(6) |
| C(1)–N(3) | 1.327(6) | | |
| O(1)–Zn(1)–O(2) | 113.7(1) | O(1)–Zn(1)–O(3) | 109.3(1) |
| O(2)–Zn(1)–O(3) | 103.6(1) | O(1)–Zn(1)–O(4) | 104.3(1) |
| O(2)–Zn(1)–O(4) | 112.6(1) | O(3)–Zn(1)–O(4) | 113.6(1) |
| O(5)–Zn(2)–O(6) | 108.9(1) | O(5)–Zn(2)–O(7) | 119.5(1) |
| O(6)–Zn(2)–O(7) | 104.5(1) | O(5)–Zn(2)–O(8) | 102.9(1) |
| O(6)–Zn(2)–O(8) | 106.1(1) | O(7)–Zn(2)–O(8) | 114.2(1) |
| O(1)–P(1)–O(3) | 113.2(2) | O(1)–P(1)–O(4) | 109.0(1) |
| O(3)–P(1)–O(4) | 112.2(2) | O(1)–P(1)–O(9) | 108.6(2) |
| O(3)–P(1)–O(9) | 103.5(2) | O(4)–P(1)–O(9) | 110.1(2) |
| O(5)–P(2)–O(6) | 113.3(2) | O(5)–P(2)–O(7) | 112.0(2) |
| O(6)–P(2)–O(7) | 108.4(1) | O(5)–P(2)–O(10) | 103.9(2) |
| O(6)–P(2)–O(10) | 109.2(2) | O(7)–P(2)–O(10) | 109.9(2) |
| O(2)–P(3)–O(8) | 116.7(2) | O(2)–P(3)–O(11) | 110.5(2) |
| O(8)–P(3)–O(11) | 105.3(2) | O(2)–P(3)–O(12) | 104.4(2) |
| O(8)–P(3)–O(12) | 110.9(2) | O(11)–P(3)–O(12) | 108.9(2) |
| Zn(1)–O(1)–P(1) | 124.0(1) | Zn(1)–O(2)–P(3) | 135.5(2) |
| Zn(1)–O(3)–P(1) | 150.2(2) | Zn(1)–O(4)–P(1) | 126.0(2) |
| Zn(2)–O(5)–P(2) | 144.4(2) | Zn(2)–O(6)–P(2) | 128.1(2) |
| Zn(2)–O(7)–P(2) | 125.6(2) | Zn(2)–O(8)–P(3) | 139.6(2) |

neighbors and an average Zn–O–P bond angle of 134.2° results from a fairly wide spread of angles (Table 4). These geometrical data are in good agreement with the results of previous structure determinations on similar compounds.¹⁰ There are three crystallographically distinct PO_4 tetrahedra in $\text{CN}_3\text{H}_6 \cdot \text{Zn}_2(\text{HPO}_4)_2\text{H}_2\text{PO}_4$: Two of these phosphate entities [P atoms P(1) and P(2)] make three P–O–Zn bonds and possess one terminal P–O bond. P(3) makes two P–O–Zn links and has two uncoordinated oxygen atom neighbors. Average P–O bond distances of 1.535(2), 1.534(2), and 1.533(2) Å result for P(1), P(2), and P(3), respectively. Assuming the usual valences of Zn, P, and O, the framework stoichiometry of $\text{Zn}_2\text{P}_3\text{O}_{12}$ in $\text{CN}_3\text{H}_6 \cdot \text{Zn}_2(\text{HPO}_4)_2\text{H}_2\text{PO}_4$ has a charge of -5 . We assume that the extraframework guanidine species is present as the singly charged guanidinium cation; thus four “framework” protons are required for charge-balancing purposes, which corresponds to the four proton sites located in Fourier maps, one of which is associated with each terminal P–O moiety, i.e., two HPO_4 groups and one H_2PO_4 group. This assignment is also consistent with the P–O bond lengths of the oxygen atoms involved [O(9)–O(12)] which show characteristic values in the range ~ 1.56 – 1.60 Å.²⁹ It would be difficult to envisage a structural model that involves five framework protons and a neutral guanidine (as opposed to guanidinium cation) extraframework species. All the (di)hydrogen phosphate protons are involved in intraframework hydrogen bonds as shown in Figure 2: O(9)–H(9)···O(4) ($d = 1.76$ Å), O(10)–H(10)···O(7) ($d = 1.78$ Å), O(11)–H(11)···O(1) ($d = 1.77$ Å), O(12)–H(12)···O(6) ($d = 1.72$ Å) with the H-bonding distances based on the restrained refinement of the framework H atoms as described above.

The polyhedral connectivity in $\text{CN}_3\text{H}_6 \cdot \text{Zn}_2(\text{HPO}_4)_2\text{H}_2\text{PO}_4$ leads to the open-framework network shown in Figure 2. ZnO_4 and HPO_4 groups are arranged in sheets lying perpendicular to the crystallographic c direction. These sheets (Figure 3) consist of 6-rings of tetrahedra, with the Zn and P species strictly alternating—there are no Zn–O–Zn or P–O–P linkages in this structure. An intrasheet H-bond is apparent in each 6-ring. There are two very similar, but crystallographically distinct sheets; at $z \approx 1/2$ (atoms Zn(1), P(1), etc.) and $z \approx 0$ (atoms Zn(2), P(2), etc.), as indicated in Figure 3. The doubled repeat pattern arises from the “ordering” of the guanidinium cations in the [100] channels (Figure 2). The Zn(1)/P(1) and Zn(2)/P(2) sheets are linked into a three-dimensional framework by the $\text{H}_2\text{P}(3)\text{O}_4$ group, in the c -direction. This polyhedral connectivity of two zinc-centered tetrahedra and three phosphorus-centered tetrahedra results in an extraframework channel system of 12-rings along [100] (approximate atom-to-atom dimensions = 6.8×6.1 Å) and squashed 8-rings along [010].

The guanidinium cations occupy the [100] channels (Figure 2). Two of the hydrogen atoms associated with this guanidinium cation were located from Fourier difference maps; the remaining four were located geometrically by assuming planar sp^2 hybridization about the remaining two N atoms. On the basis of this assumption, five hydrogen-bonding links are made by the guanidinium cation's N–H groups, as N(1)–H(1)···O(5) [$d = 2.23$ Å]; N(2)–H(3)···O(8) [$d = 2.27$ Å]; N(2)–H(4)···O(9) [$d = 2.06$ Å]; N(3)–H(5)···O(2) [$d = 2.31$ Å]; N(3)–H(6)···O(3) [$d = 2.31$ Å]. On average, these template–framework N–H···O hydrogen bonds are substantially longer than the intraframework O–H···O links noted above.

Crystal Structure of $(\text{CN}_3\text{H}_6)_2 \cdot \text{Zn}(\text{HPO}_4)_2$: This phase consists of an anionic zincophosphate framework of unprecedentedly low framework atom density (vide infra), enclosing an intersecting two-dimensional network of channels, occupied by guanidinium cations. Final atomic coordinates and thermal parameters for $(\text{CN}_3\text{H}_6)_2 \cdot \text{Zn}(\text{HPO}_4)_2$ are presented in Table 5, with selected geometrical data in Table 6. The building unit of $(\text{CN}_3\text{H}_6)_2 \cdot \text{Zn}(\text{HPO}_4)_2$ is shown in Figure 4.

The single distinct zinc atom in $(\text{CN}_3\text{H}_6)_2 \cdot \text{Zn}(\text{HPO}_4)_2$ is tetrahedrally coordinated to oxygen with an average Zn–O bond distance of 1.943(2) Å. This zinc atom makes four Zn–O–P bonds to four distinct P atom neighbors resulting in an average Zn–O–P bond angle of 125.7°. There are two crystallographically distinct phosphate tetrahedra in $(\text{CN}_3\text{H}_6)_2 \cdot \text{Zn}(\text{HPO}_4)_2$: Both of these groups make two bonds to adjacent Zn atoms and possess two terminal P–O bonds. Average P–O bond distances of 1.536(2) Å result for both P(1) and P(2). The resulting ZnP_2O_8 framework stoichiometry has a charge of -4 . In this material, there are two extraframework guanidinium cations, thus two “framework” protons are required for charge-balancing purposes. One of these, attached to O(5), was located in Fourier difference maps, and the other [attached to O(8)] may be located on the basis of the uncoordinated P–O bond lengths, as noted above, i.e., there are two HPO_4 groups in $(\text{CN}_3\text{H}_6)_2 \cdot \text{Zn}(\text{HPO}_4)_2$. The proton attached to O(5) is involved in a strong H-bonding interaction as O(5)–H(1)···O(7) ($d = 1.58$ Å) based on the restrained refinement of the H

(29) Lightfoot, P.; Masson, D. *Acta Crystallogr.* **1996**, *C52*, 1077.

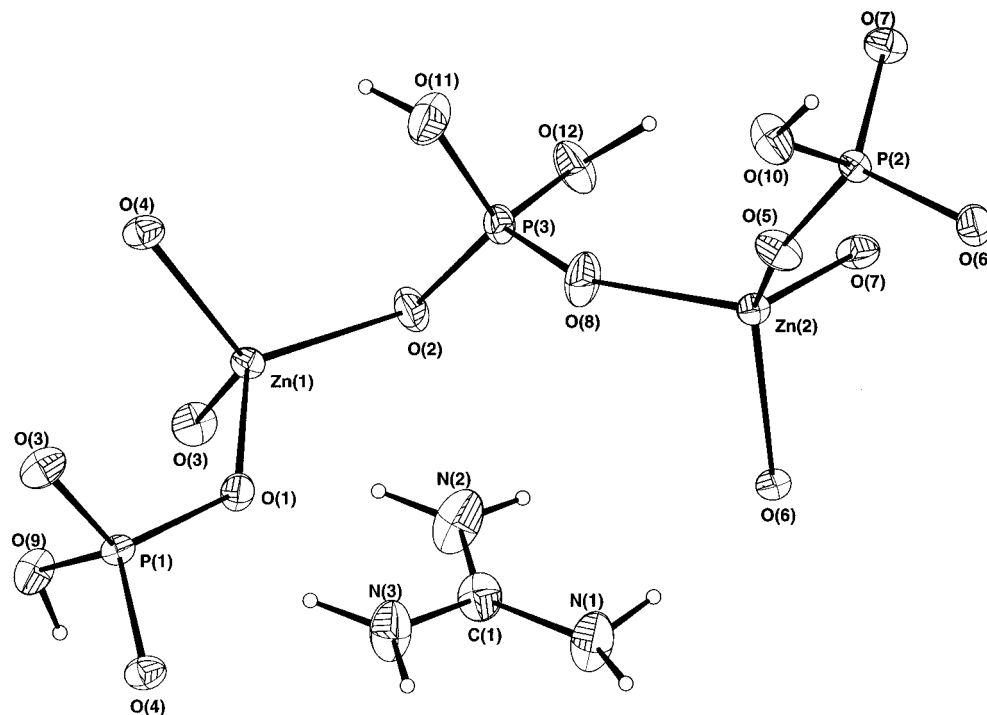


Figure 1. View of a fragment of the crystal structure of $\text{CN}_3\text{H}_6 \cdot \text{Zn}_2(\text{HPO}_4)_2\text{H}_2\text{PO}_4$ showing the atom-labeling scheme (50% thermal ellipsoids; protons represented by spheres of arbitrary radius).

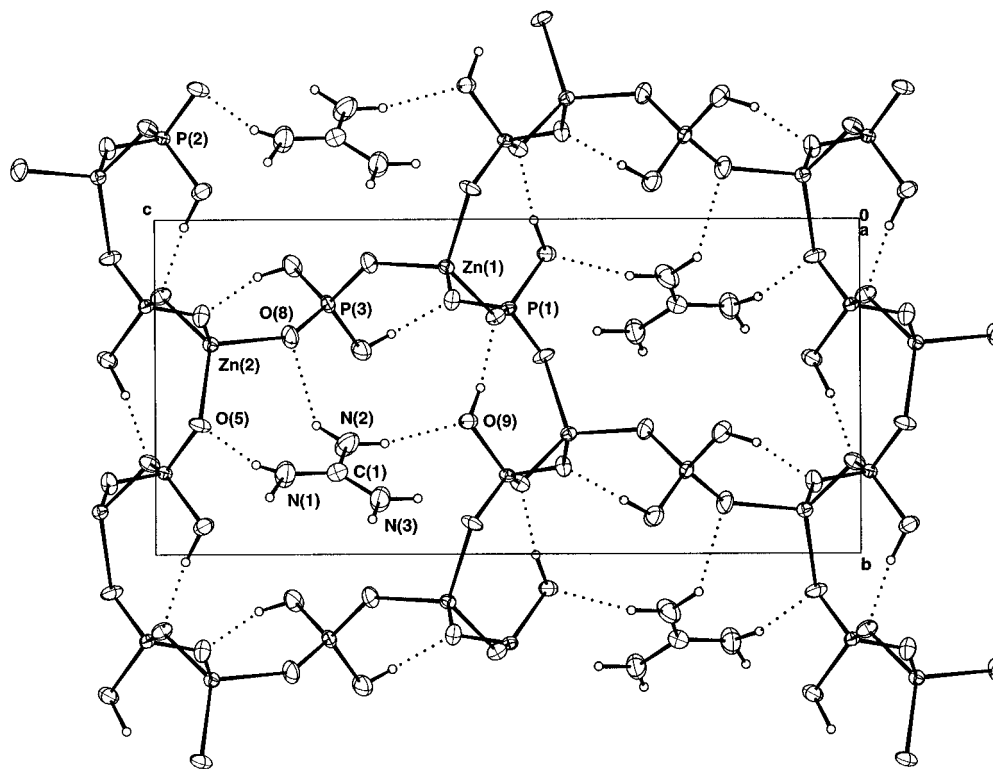


Figure 2. View down [100] of the crystal structure of $\text{CN}_3\text{H}_6 \cdot \text{Zn}_2(\text{HPO}_4)_2\text{H}_2\text{PO}_4$ showing the one-dimensional 12-ring channel system occupied by guanidinium cations. Possible hydrogen-bonding links are indicated by dotted lines.

atoms as described above; O(8) has several suitable nonbonded contacts to nearby oxygen atoms to accommodate a possible $\text{O}(8)\text{--H}\cdots\text{O}$ hydrogen bond.

The polyhedral connectivity in $(\text{CN}_3\text{H}_6)_2 \cdot \text{Zn}(\text{HPO}_4)_2$ leads to a new open-framework topology. Vertex-sharing helical chains of $\text{Zn}(1)\text{O}_4$ and $\text{HP}(1)\text{O}_4$ groups propagate in the polar c unit-cell direction. The zinc nodes of these chains are cross-linked by the $\text{HP}(2)\text{O}_4$ moieties in the a direction. As with $\text{CN}_3\text{H}_6 \cdot \text{Zn}_2$

$(\text{HPO}_4)_2\text{H}_2\text{PO}_4$, there are no Zn--O--Zn or P--O--P links in this structure. This polyhedral connectivity of one zinc-centered tetrahedron and two phosphorus-centered tetrahedra results in a striking channel system of intersecting 12-rings which propagate in the [100] and [001] directions (Figures 5 and 6). Conversely, no channels are apparent in this structure when viewed down [010]. The smallest identifiable ring system in this topology is a 12-ring for both Zn and P.

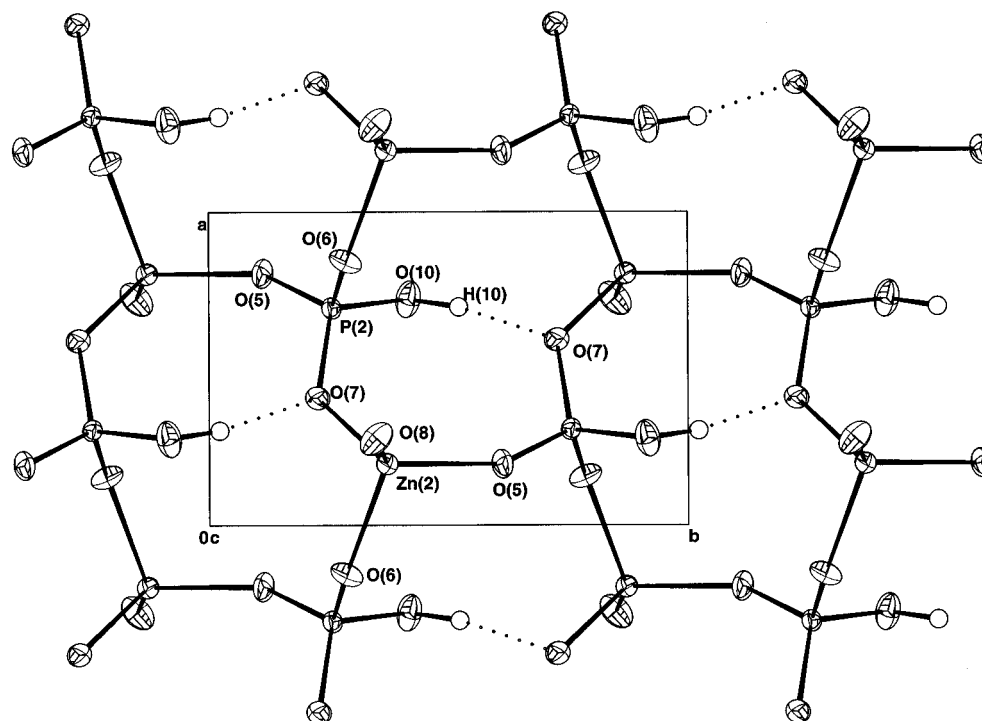


Figure 3. View down [001] of part of a $\text{Zn}(\text{HPO}_4)$ sheet in the $\text{CN}_3\text{H}_6 \cdot \text{Zn}_2(\text{HPO}_4)_2 \cdot \text{H}_2\text{PO}_4$ structure. Note the in-sheet H-bonding linkage.

Table 5. Final Atomic Coordinates/Thermal Factors for $(\text{CN}_3\text{H}_6)_2 \cdot \text{Zn}(\text{HPO}_4)_2$

| atom | <i>x</i> | <i>y</i> | <i>z</i> | U_{eq}^a |
|-------|------------|------------|------------|-------------------|
| Zn(1) | 0.01878(4) | 0.13320(4) | 0.3155(1) | 0.0158 |
| P(1) | -0.0022(1) | 0.01654(9) | 0.0549(2) | 0.0178 |
| P(2) | 0.2674(1) | 0.25549(9) | 0.2246(2) | 0.0165 |
| O(1) | 0.1872(3) | 0.1974(2) | 0.3270(4) | 0.0217 |
| O(2) | -0.0908(3) | 0.2525(2) | 0.2608(3) | 0.0200 |
| O(3) | 0.0275(3) | 0.0077(2) | 0.2009(3) | 0.0205 |
| O(4) | -0.0370(3) | 0.0886(3) | 0.4879(4) | 0.0247 |
| O(5) | -0.1522(3) | 0.0238(3) | 0.0371(4) | 0.0294 |
| O(6) | 0.0593(4) | 0.1161(3) | -0.0027(4) | 0.0336 |
| O(7) | 0.2259(3) | 0.3734(2) | 0.2086(4) | 0.0249 |
| O(8) | 0.2549(3) | 0.1976(3) | 0.0892(4) | 0.0274 |
| C(1) | 0.2658(5) | -0.2340(4) | 0.2120(6) | 0.0305 |
| N(1) | 0.2044(5) | -0.1780(4) | 0.3019(6) | 0.0422 |
| N(2) | 0.2360(5) | -0.2217(5) | 0.0873(5) | 0.0417 |
| N(3) | 0.3531(5) | -0.3049(4) | 0.2468(5) | 0.0475 |
| C(2) | 0.4885(5) | 0.0184(5) | -0.0475(6) | 0.0364 |
| N(4) | 0.5130(4) | 0.0976(4) | 0.0350(6) | 0.0415 |
| N(5) | 0.5782(5) | -0.0479(4) | -0.0859(6) | 0.0444 |
| N(6) | 0.3695(5) | 0.0053(4) | -0.0931(6) | 0.0458 |

$$^a U_{\text{eq}} (\text{\AA}^2) = \frac{1}{3} [U_1 + U_2 + U_3].$$

The guanidinium cations occupy the channels in $(\text{CN}_3\text{H}_6)_2 \cdot \text{Zn}(\text{HPO}_4)_2$, with the C(1)-centered species appearing to occupy the [100] channels, and the C(2)-centered species occupying the [010] channels. Both channels have approximate dimensions of $7.6 \times 8.2 \text{ \AA}$ when measured from O atom to O atom. A more detailed view of the possible hydrogen-bonding configuration of one of the guanidinium species is shown in Figure 7. It appears that the guanidinium cation is acting to template the resulting 12-ring of alternating Zn- and P-centered tetrahedral nodes, with N-H...O hydrogen bonding playing an important role. One of the template-framework hydrogen-bonding links involves an Zn-O-P bridge; the remainder involve terminal P-O (or P-OH) links. The spread of template-framework H-bonding contact distances in $\text{CN}_3\text{H}_6 \cdot$

Table 6. Selected Bond Distances (\AA) and Angles (deg) for $(\text{CN}_3\text{H}_6)_2 \cdot \text{Zn}(\text{HPO}_4)_2$

| | | | |
|-----------------|----------|-----------------|----------|
| Zn(1)-O(1) | 1.934(3) | Zn(1)-O(2) | 1.948(3) |
| Zn(1)-O(3) | 1.945(3) | Zn(1)-O(4) | 1.937(4) |
| P(1)-O(3) | 1.529(4) | P(1)-O(4) | 1.524(4) |
| P(1)-O(5) | 1.580(4) | P(1)-O(6) | 1.507(4) |
| P(2)-O(1) | 1.520(4) | P(2)-O(2) | 1.530(3) |
| P(2)-O(7) | 1.528(3) | P(2)-O(8) | 1.564(4) |
| C(1)-N(1) | 1.317(7) | C(1)-N(2) | 1.321(7) |
| C(1)-N(3) | 1.313(6) | C(2)-N(4) | 1.317(7) |
| C(2)-N(5) | 1.305(7) | C(2)-N(6) | 1.338(7) |
| O(1)-Zn(1)-O(2) | 104.0(1) | O(1)-Zn(1)-O(3) | 108.7(1) |
| O(2)-Zn(1)-O(3) | 117.2(1) | O(1)-Zn(1)-O(4) | 109.6(2) |
| O(2)-Zn(1)-O(4) | 107.4(1) | O(3)-Zn(1)-O(4) | 109.6(1) |
| O(3)-P(1)-O(4) | 108.9(2) | O(3)-P(1)-O(5) | 108.5(2) |
| O(4)-P(1)-O(5) | 105.2(2) | O(3)-P(1)-O(6) | 110.7(2) |
| O(4)-P(1)-O(6) | 113.8(2) | O(5)-P(1)-O(6) | 109.4(2) |
| O(1)-P(2)-O(2) | 109.7(2) | O(1)-P(2)-O(7) | 111.5(2) |
| O(2)-P(2)-O(7) | 111.2(2) | O(1)-P(2)-O(8) | 110.4(2) |
| O(2)-P(2)-O(8) | 105.4(2) | O(7)-P(2)-O(8) | 108.5(2) |
| Zn(1)-O(1)-P(2) | 130.8(3) | Zn(1)-O(2)-P(2) | 126.1(2) |
| Zn(1)-O(3)-P(1) | 121.5(2) | Zn(1)-O(4)-P(1) | 124.8(2) |

$\text{Zn}_2(\text{HPO}_4)_2 \cdot \text{H}_2\text{PO}_4$ covers the range $\sim 1.90\text{--}2.29 \text{ \AA}$, based on geometrical placement and restrained refinement of the hydrogen atoms of the guanidinium cations.

Crystal Structure of $(\text{CN}_3\text{H}_6)_6 \cdot \text{Zn}_2(\text{OH})(\text{PO}_4)_3 \cdot \text{H}_2\text{O}$.

This material adopts a completely different crystal structure to its partners and is built up from one-dimensional chains of vertex-sharing ZnO_4 and PO_4 units (Figure 8). Final atomic positional and thermal parameters are presented in Table 7 with selected geometrical data in Table 8.

The two zinc atoms in $(\text{CN}_3\text{H}_6)_6 \cdot \text{Zn}_2(\text{OH})(\text{PO}_4)_3 \cdot \text{H}_2\text{O}$ are both nominally tetrahedrally coordinated but are significantly distorted and could almost be described as triangular-based pyramidal (Figure 8). Each zinc center makes three Zn-O-P bonds to different P atoms ($\theta_{\text{av}} = 136.4^\circ$) and one Zn-OH-Zn link, which is nominally linear. The single phosphate group in $(\text{CN}_3\text{H}_6)_6 \cdot \text{Zn}_2(\text{OH})(\text{PO}_4)_3 \cdot \text{H}_2\text{O}$ is involved in two P-O-Zn linkages

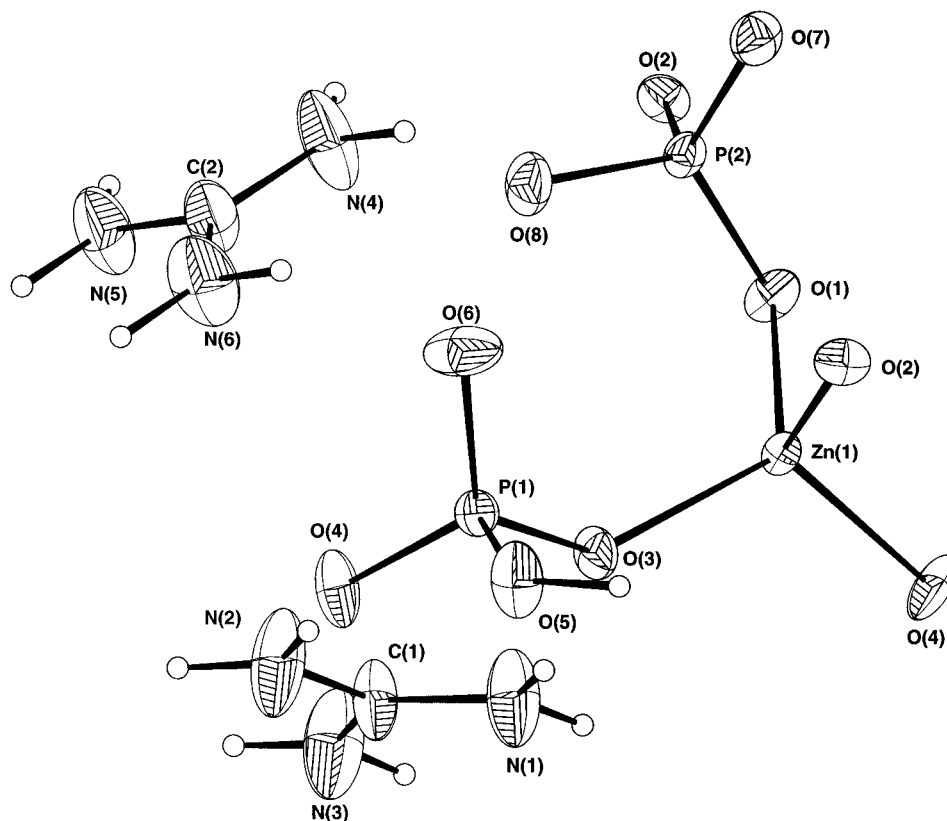


Figure 4. View of a fragment of the $(\text{CN}_3\text{H}_6)_2\cdot\text{Zn}(\text{HPO}_4)_2$ crystal structure showing the atom-labeling scheme (50% thermal ellipsoids; protons represented by spheres of arbitrary radius).

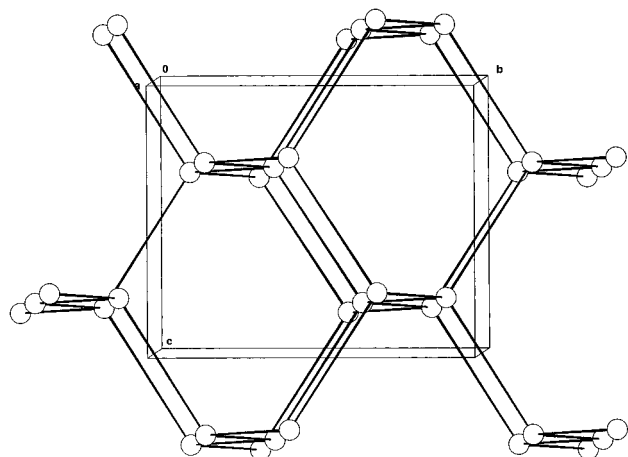


Figure 5. Skeletal representation, viewed approximately down $[100]$, of the ZnPO framework connectivity in $(\text{CN}_3\text{H}_6)_2\cdot\text{Zn}(\text{HPO}_4)_2$, showing the 12-ring channels (see text). In this diagram, plain spheres represent Zn atoms, with lines showing their topological connectivity. Note that these lines represent intervening HPO_4 groups and not simply intervening O atoms. Thus, a “six-ring” of Zn atoms corresponds to a 12-ring of tetrahedral nodes (6 Zn and 6 P), or 24 atoms (6 Zn, 6 P, 12 O) in total.

[via O(1) and O(2)] and two terminal P–O bonds. These short ($d < 1.52 \text{ \AA}$) terminal bonds to O(3) and O(4) indicate that they are not protonated, i.e., this is a simple phosphate group. There are no P–O–P bonds in this structure. The skeletal stoichiometry of $\text{Zn}_2\text{P}_3\text{O}_{13}$ in $(\text{CN}_3\text{H}_6)_6\cdot\text{Zn}_2(\text{OH})(\text{PO}_4)_3\cdot\text{H}_2\text{O}$ has a charge of -7 ; six guanidinium cations are present, thus one skeletal proton is required, which we suggest is located on the inter-zinc bridging oxygen atom, i.e., a bridging hydrox-

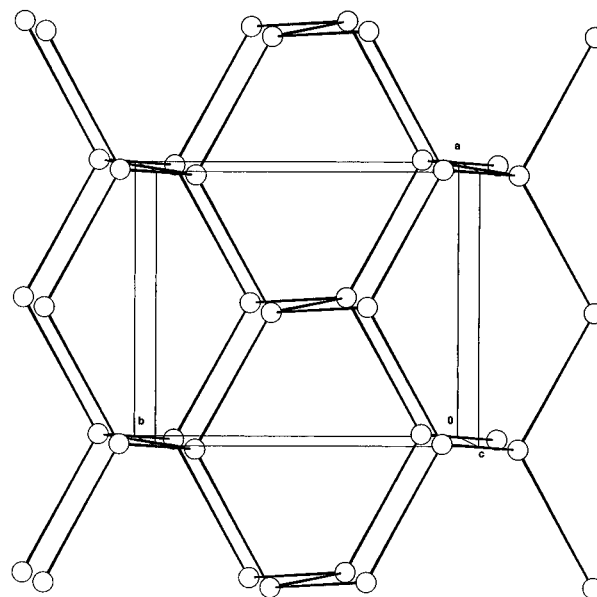


Figure 6. Skeletal view approximately down $[001]$ of the second 12-ring channel system in $(\text{CN}_3\text{H}_6)_2\cdot\text{Zn}(\text{HPO}_4)_2$ (compare Figure 5).

ide group. Crystal symmetry dictates the presence of two of these OH groups per asymmetric unit.

The Zn/P/O connectivity in $(\text{CN}_3\text{H}_6)_6\cdot\text{Zn}_2(\text{OH})(\text{PO}_4)_3\cdot\text{H}_2\text{O}$ results in infinite chains propagating along the c direction. A structural *motif* in which two zinc-centered tetrahedra are bridged by *three* phosphate groups is apparent (Figure 8), which, so far as we are aware, has not been previously observed in simple “inorganic” phosphate-containing chains constructed from tetrahedral building units. These triply bridged units are linked together via hydroxide groups, resulting

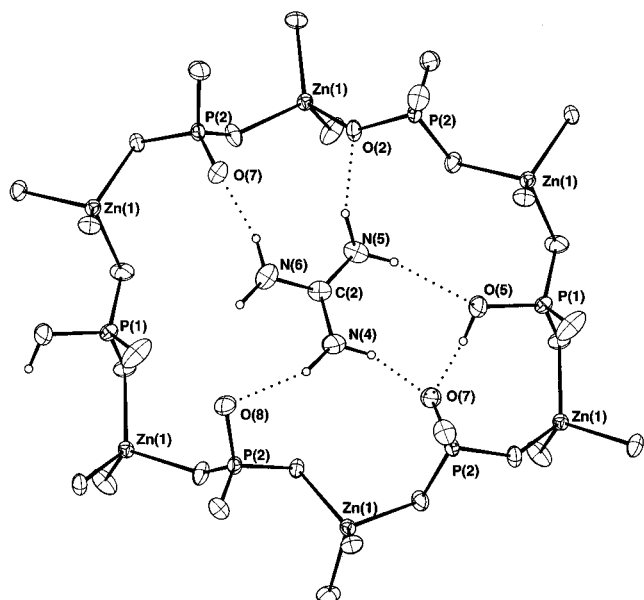


Figure 7. Detail of the $(\text{CN}_3\text{H}_6)_2 \cdot \text{Zn}(\text{HPO}_4)_2$ structure showing the templating effect of the C(2)-centered guanidinium cation in occupying a framework tetrahedral 12-ring. Possible hydrogen bonding links are indicated by dotted lines. Note the intraframework H bond.

Table 7. Final Atomic Coordinates/Thermal Factors for $(\text{CN}_3\text{H}_6)_6 \cdot \text{Zn}_2(\text{OH})(\text{PO}_4)_3 \cdot \text{H}_2\text{O}$

| atom | x | y | z | U_{eq}^a |
|-------|------------|-----------|-----------|----------------------|
| Zn(1) | 0 | 0 | 0.3651(2) | 0.0175 |
| Zn(2) | 0 | 0 | 0.1350(2) | 0.0180 |
| P(1) | -0.1043(3) | 0.0541(3) | 0.2499(3) | 0.0236 |
| O(1) | 0.1060(6) | 0.0733(6) | 0.1587(8) | 0.0359 |
| O(2) | -0.0766(6) | 0.0276(6) | 0.3377(8) | 0.0365 |
| O(3) | -0.1915(6) | 0.0097(6) | 0.2465(7) | 0.0278 |
| O(4) | -0.0725(6) | 0.1400(6) | 0.2542(7) | 0.0311 |
| O(5) | 0 | 0 | 0 | 0.09(1) ^b |
| O(6) | 0 | 0 | 1/2 | 0.06(1) ^b |
| O(10) | 0.5153(7) | 0.4138(7) | 0.1120(8) | 0.0505 |
| C(1) | 0.252(1) | 0.046(1) | 0.006(2) | 0.0272 |
| N(1) | 0.1785(8) | 0.0211(9) | 0.009(1) | 0.0244 |
| N(2) | 0.2846(8) | 0.0392(8) | -0.075(1) | 0.0398 |
| N(3) | 0.2967(8) | 0.0763(8) | 0.084(1) | 0.0275 |
| C(2) | 0.476(1) | 0.086(1) | -0.168(2) | 0.0341 |
| N(4) | 0.4542(8) | 0.0539(8) | -0.079(1) | 0.0388 |
| N(5) | 0.4645(8) | 0.0379(8) | -0.240(1) | 0.0346 |
| N(6) | 0.5026(8) | 0.1599(9) | -0.180(1) | 0.0337 |

^a $U_{\text{eq}} (\text{\AA}^2) = 1/3[U_1 + U_2 + U_3]$. ^b $U_{\text{iso}} (\text{\AA}^2)$.

Table 8. Selected Bond Distances (Å) and Angles (deg) for $(\text{CN}_3\text{H}_6)_6 \cdot \text{Zn}_2(\text{OH})(\text{PO}_4)_3 \cdot \text{H}_2\text{O}$

| | | | |
|------------------|----------|------------------|----------|
| Zn(1)–O(2) × 3 | 1.91(1) | Zn(1)–O(6) | 1.883(3) |
| Zn(2)–O(1) × 3 | 1.91(1) | Zn(2)–O(5) | 1.884(3) |
| P(1)–O(1) | 1.57(1) | P(1)–O(2) | 1.54(1) |
| P(1)–O(3) | 1.51(1) | P(1)–O(4) | 1.51(1) |
| C(1)–N(1) | 1.30(2) | C(1)–N(2) | 1.34(2) |
| C(1)–N(3) | 1.34(2) | C(2)–N(4) | 1.36(2) |
| C(2)–N(5) | 1.33(2) | C(2)–N(6) | 1.31(2) |
| O(2)–Zn(1)–O(2) | 116.1(2) | O(2)–Zn(1)–O(6) | 101.5(3) |
| O(1)–Zn(2)–O(1) | 117.1(2) | O(1)–Zn(2)–O(5) | 100.0(3) |
| O(1)–P(1)–O(2) | 106.9(6) | O(1)–P(1)–O(3) | 108.2(7) |
| O(2)–P(1)–O(3) | 109.3(6) | O(1)–P(1)–O(4) | 110.1(6) |
| O(2)–P(1)–O(4) | 110.0(6) | O(3)–P(1)–O(4) | 112.2(6) |
| Zn(2)–O(1)–P(1) | 135.3(7) | Zn(1)–O(2)–P(1) | 137.4(7) |
| Zn(2)–O(5)–Zn(2) | 180 | Zn(1)–O(6)–Zn(1) | 180 |

in 180° Zn–O–Zn bond angles, as modeled in the crystal structure refinement which is constrained by the 3-fold symmetry of the Zn–O–Zn axis. As with the case of aluminosilicates, this linear intertetrahedral bond con-

figuration is considered to be energetically unfavorable³⁰ and the real situation almost certainly involves a reduction in the bond angle by the bending of the Zn–O–Zn bond away from the 3-fold axis. This is supported by the fact that anisotropic refinement of the bridging atoms O(5) and O(6) resulted in nonpositive definite thermal factors, indicative of a “smearing” of scattering density around the 3-fold axis. Attempts to model this effect by shifting the bridging O atoms to partially occupied sites around the 3-fold axis led to unstable refinements, perhaps due to the limitations of the data set for this material, as noted above.

The guanidinium cations interact with the $[\text{Zn}_2(\text{OH})(\text{PO}_4)_3]^{6-}$ chains through a complex network of H-bonds (Figure 9), involving both terminal P–O and bridging Zn–O–P oxygen atom species as acceptors. One of the two crystallographically distinct guanidinium cations [central carbon atom C(1)] serves to cross-link adjacent zincophosphate chains; the other [carbon atom C(2)] makes links to one chain and also interacts with the extraframework water molecule. Both guanidinium cations make five N–H···O hydrogen bonding interactions, with hydrogen–oxygen contact distances ranging from ~1.90 to 2.20 Å.

Discussion

Three new guanidinium zinc phosphate phases, $\text{CN}_3\text{H}_6 \cdot \text{Zn}_2(\text{HPO}_4)_2\text{H}_2\text{PO}_4$, $(\text{CN}_3\text{H}_6)_2 \cdot \text{Zn}(\text{HPO}_4)_2$, and $(\text{CN}_3\text{H}_6)_6 \cdot \text{Zn}_2(\text{OH})(\text{PO}_4)_3 \cdot \text{H}_2\text{O}$, have been prepared as single crystals by a simple synthetic procedure and characterized by single-crystal diffraction methods. They are built up from the expected tetrahedral building blocks of ZnO_4 and PO_4 units, sharing vertexes, but the three new structures that result are quite distinct from each other. As is typical of kinetically controlled solvent-mediated reactions, there is no particular correlation between starting composition and the majority solid-phase product stoichiometry.³¹

$\text{CN}_3\text{H}_6 \cdot \text{Zn}_2(\text{HPO}_4)_2\text{H}_2\text{PO}_4$ and $(\text{CN}_3\text{H}_6)_2 \cdot \text{Zn}(\text{HPO}_4)_2$ consist of three-dimensional networks; Zn–O–P bonds are strongly favored over possible Zn–O–Zn and P–O–P connections, despite the non-1:1 Zn:P framework ratios in these phases. This results in either one or two terminal P–O bonds for the phosphate moieties, some of which are protonated. A plausible scheme for locating the framework P–OH protons was possible on the basis of charge-balancing and geometrical criteria. One may ask why these framework protons arise, as opposed to possible continuous (all O atoms forming Zn–O–P bridges) networks, which are known to be feasible for several open-framework zincophosphates templated by alkali metals.⁹ It is possible that a continuous, fully ordered 1:1 Zn:P framework is difficult to achieve in the organically templated materials because of the difficulty of packing enough bulky *organic cations* into the extraframework pores to achieve charge balance. Unlike many aluminosilicates, in which the Si:Al ratio is variable, and affects the charge-balancing requirement, ZnPOs all appear to have a precisely defined Zn:P ratio for a particular structural topology. We note that inclusion of (di)hydrogen phosphate protons reduces the

(30) Hill, R. J.; Gibbs, G. V. *Acta Crystallogr.* **1979**, B35, 25.

(31) Harrison, W. T. A.; Dussack, L. L.; Jacobson, A. J. *J. Solid State Chem.* **1996**, 125, 234.

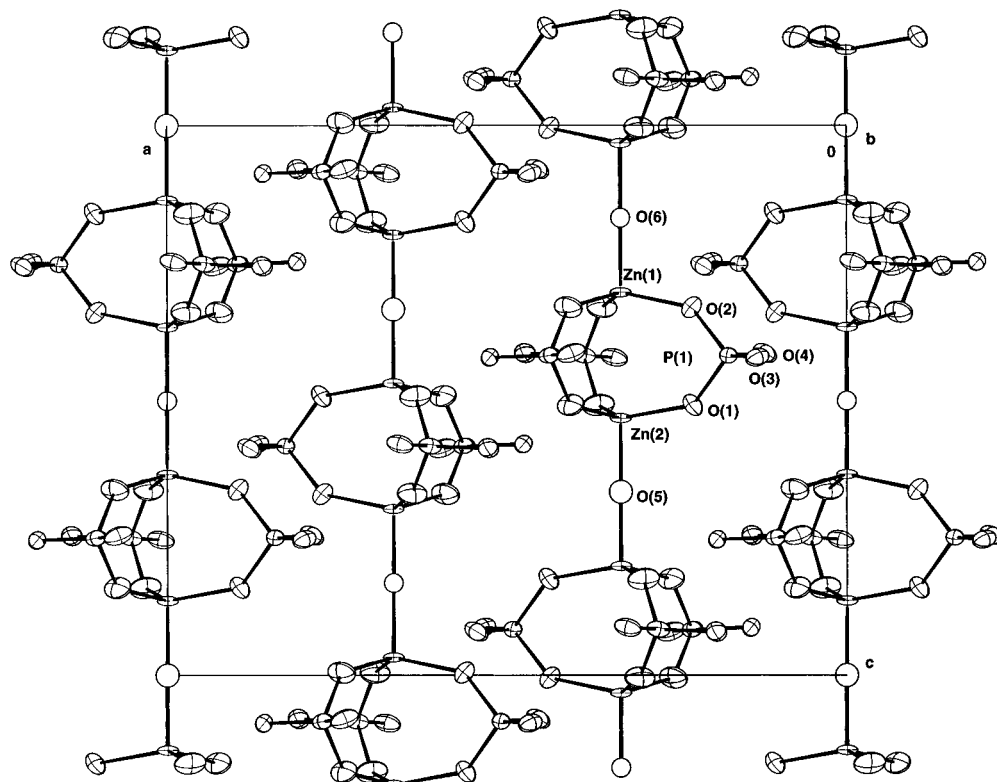


Figure 8. View down [010] of the $(\text{CN}_3\text{H}_6)_6 \cdot \text{Zn}_2(\text{OH})(\text{PO}_4)_3 \cdot \text{H}_2\text{O}$ structure showing isolated, one-dimensional $\text{Zn}_2(\text{OH})(\text{PO}_4)_3$ columns propagating along [001]. Guanidinium cations and extraframework water molecules omitted for clarity (50% thermal ellipsoids).

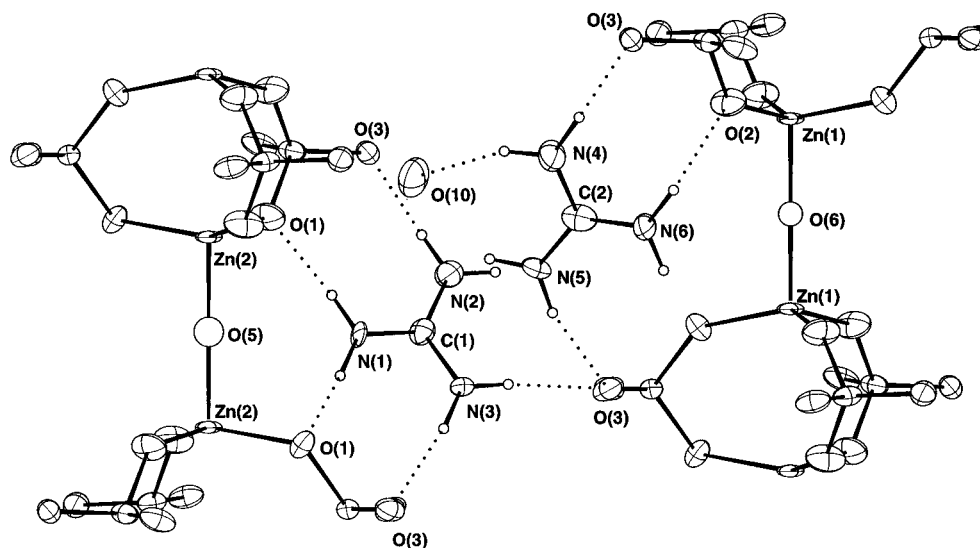


Figure 9. Detail of the $(\text{CN}_3\text{H}_6)_6 \cdot \text{Zn}_2(\text{OH})(\text{PO}_4)_3 \cdot \text{H}_2\text{O}$ structure showing intercolumn hydrogen-bonding connectivity via the guanidinium cations. Note that one guanidinium cation [carbon atom C(2) etc.] also bonds to the extraframework water molecule, O(10).

anionic framework charge density in $\text{CN}_3\text{H}_6 \cdot \text{Zn}_2(\text{HPO}_4)_2\text{H}_2\text{PO}_4$ from $-7.52 \text{ e}/1000 \text{ \AA}^3$ to $-1.51 \text{ e}/1000 \text{ \AA}^3$. Continuous-framework zincophosphates templated by metal cations have significantly higher framework charge densities of up to $-8 \text{ e}/1000 \text{ \AA}^3$, which are essentially the same as those of their aluminosilicate isostructures.

On the basis of the structures of $\text{CN}_3\text{H}_6 \cdot \text{Zn}_2(\text{HPO}_4)_2\text{H}_2\text{PO}_4$ and $(\text{CN}_3\text{H}_6)_2 \cdot \text{Zn}(\text{HPO}_4)_2$ [but not that of $(\text{CN}_3\text{H}_6)_6 \cdot \text{Zn}_2(\text{OH})(\text{PO}_4)_3 \cdot \text{H}_2\text{O}$], we may tentatively propose a structure-directing effect for the guanidinium cation with respect to zincophosphate networks. This cation appears to preferentially template a tetrahedral 12-ring framework *motif* and adopts a side-on orientation as

suggested above and presumably forms longish, but structurally significant N–H···O hydrogen bonding linkages. However, we stress that *intraframework* hydrogen bonds, and the constraints imposed by the fixed Zn:P ratio in terms of preference for Zn–O–P and avoidance of Zn–O–Zn and P–O–P bonds are also clearly important in determining the three-dimensional frameworks of these materials. This distantly relates to Löwenstein's rule for the avoidance of Al–O–Al linkages in aluminosilicates,³² but the similarity should not be overstressed, because zincophosphates never show any long-range Zn/P site mixing akin to Al/Si

(32) Löwenstein, W. *Am. Miner.* **1954**, *39*, 92.

disorder commonly observed in aluminosilicates. Thus, the *local* templating effect of the guanidinium cation cannot be simply correlated with the resulting overall crystal structures. In the novel phase $(\text{CN}_3\text{H}_6)_3\cdot\text{Zn}_7\cdot(\text{H}_2\text{O})_4(\text{PO}_4)_6\cdot\text{H}_3\text{O}$ the guanidinium cations also template 12-rings via structurally important $\text{N}-\text{H}\cdots\text{O}$ hydrogen-bonding linkages, but also show a remarkable “cooperative” effect to result in a group of three CN_3H_6^+ cations templating an 18-ring cavity in “side-by-side” configuration.²⁰

A useful parameter for quantifying the “openness” of molecular sieve structures is the framework density (FD)—the number of framework tetrahedral (*T*) atoms (here: Zn and P) per unit volume.³³ For $\text{CN}_3\text{H}_6\cdot\text{Zn}_2(\text{HPO}_4)_2\text{H}_2\text{PO}_4$, a FD value of 15.1 *T*-atoms/1000 Å³ results, which is in the middle of the range of FD values observed for aluminosilicate zeolites.³⁴ Conversely, $(\text{CN}_3\text{H}_6)_2\cdot\text{Zn}(\text{HPO}_4)_2$ has a remarkably low FD value of 9.10 *T*-atoms/1000 Å³, which appears to be the lowest FD value yet observed for a microporous material. Comparable FD values of 12.7 *T*-atoms/1000 Å³ for aluminosilicate faujasite, and 11.1 *T*-atoms/1000 Å³ for the interrupted tetrahedral gallofluorophosphate framework in cloverite result.³⁴ $\text{Cs}_3[\text{V}_5\text{O}_9(\text{PO}_4)_2]\cdot x\text{H}_2\text{O}$, which contains a remarkable “diamond”-like 3-dimensional array of spheroidal 32-ring cavities⁸ has a FD value of ~9.3 nodal atoms/1000 Å³ (square-pyramidal V atoms, tetrahedral P atoms). Another way to quantify the openness of these types of materials is to calculate the fraction of the unit cell volume *not* occupied by the framework (Zn, P, and O) atoms, assuming typical van der Waals’ radii for these species. The CALC SOLV option (default settings) of the program PLATON97³⁵ indicated that 723 Å³ (55% of the unit-cell volume) could be considered as “solvent accessible” in $(\text{CN}_3\text{H}_6)_2\cdot\text{Zn}(\text{HPO}_4)_2$, when the C, N, and H atoms of the guanidinium cations were ignored. However, only 38 Å³ (3% of the unit-cell volume) remained unoccupied when the guanidinium cations were included in the calculation.

The 1:2 Zn:P ratio found in $(\text{CN}_3\text{H}_6)_2\cdot\text{Zn}(\text{HPO}_4)_2$ appears to be a fruitful one for construction of ultralow-framework atom density networks. The novel phase $\text{N}(\text{CH}_3)_4\cdot\text{ZnH}_3(\text{PO}_4)_2$ adopts a different all-12-ring topology to that of $(\text{CN}_3\text{H}_6)_2\cdot\text{Zn}(\text{HPO}_4)_2$ and has a resulting FD of ~10.1.³⁶ Interestingly, the guanidinium zinc sulfate, $(\text{CN}_3\text{H}_6)_2\cdot\text{Zn}(\text{SO}_4)_2$,³⁷ reported a number of years ago, contains an open-framework zincosulfate network (1:2 Zn:S ratio) enclosing 12-ring channels occupied by guanidinium cations.

$(\text{CN}_3\text{H}_6)_6\cdot\text{Zn}_2(\text{OH})(\text{PO}_4)_3\cdot\text{H}_2\text{O}$ adopts a “polymeric” one-dimensional structure involving three PO_4 groups triply bridging pairs of distorted Zn-centered tetrahedra. Various zinc (and other divalent metal) *phosphonates* with bulky/long-chain organic substituents such as $\text{Zn}[\text{PO}_2(n\text{-C}_4\text{H}_9)_2\text{PO}_2(n\text{-C}_6\text{H}_{13})_2]$ adopt a similar triply bridged tetrahedral chain *motif* and were structurally characterized many years ago.³⁸ $(\text{CN}_3\text{H}_6)_6\cdot\text{Zn}_2(\text{OH})(\text{PO}_4)_3\cdot\text{H}_2\text{O}$ appears to be the first simple *phosphate* to adopt this polymeric configuration, further adding to the variety of novel one-dimensional zincophosphate chain structures.³⁹ We note that $(\text{CN}_3\text{H}_6)_6\cdot\text{Zn}_2(\text{OH})(\text{PO}_4)_3\cdot\text{H}_2\text{O}$ is quite distinct from $\text{Zn}[\text{PO}_2(n\text{-C}_4\text{H}_9)_2\text{PO}_2(n\text{-C}_6\text{H}_{13})_2]$ in the polymeric linking of the triply bridged tetrahedral units: in $(\text{CN}_3\text{H}_6)_6\cdot\text{Zn}_2(\text{OH})(\text{PO}_4)_3\cdot\text{H}_2\text{O}$ the $[\text{OZn}(\text{PO}_4)_3\text{ZnO}]$ units are fused directly together, whereas in $\text{Zn}[\text{PO}_2(n\text{-C}_4\text{H}_9)_2\text{PO}_2(n\text{-C}_6\text{H}_{13})_2]$, an intermediate phosphonate group joins the nominally equivalent $[\text{OZn}(\text{PO}_2\text{R}_2)_3\text{ZnO}]$ units into a contorted polymeric strand. This also results in different Zn:P ratios for the phosphonates (Zn:P = 1:2) and phosphate (Zn:P = 2:3). It is notable that the Zn–(OH)–Zn linkage involves a hydroxide bridge in $(\text{CN}_3\text{H}_6)_6\cdot\text{Zn}_2(\text{OH})(\text{PO}_4)_3\cdot\text{H}_2\text{O}$. In $\text{Na}_2\text{ZnPO}_4\text{OH}\cdot 7\text{H}_2\text{O}$, which is built from a unique chain topology of vertex-sharing tetrahedral three-rings, a Zn–(OH)–Zn bridging link is also observed.³⁹ Any “templating” or structure-directing effect of the guanidinium cation is much harder to quantify in the $(\text{CN}_3\text{H}_6)_6\cdot\text{Zn}_2(\text{OH})(\text{PO}_4)_3\cdot\text{H}_2\text{O}$ structure although its hydrogen-bonding links, which cross-link adjacent $[\text{Zn}_2(\text{OH})(\text{PO}_4)_3]^{6-}$ chains are broadly similar in nature to those observed in the other guanidinium zinc phosphates reported here. Conceivably, this phase adopts a one-dimensional structure because its skeletal charge density of $-8.67 e/1000 \text{ \AA}^3$ (protons omitted) is too high to allow the formation of a viable three-dimensional network with sufficient empty space to accommodate the necessary number of guanidinium species for charge balancing.

Supporting Information Available: Tables of calculated atom positions and anisotropic thermal factors (6 pages); observed and calculated structure factors (32 pages). Ordering information is given on any current masthead page.

Acknowledgment. We thank Mae Lambert and Julie Anderson (SNL) for assistance. Work at UWA was supported by the Australian Research Council; work at SNL was supported by the US Department of Energy under Contract DE-AC04-94AL85000.

CM9701264

(33) Brunner, G. O.; Meier, W. M. *Nature (London)* **1989**, *337*, 146.

(34) Meier, W. M.; Olson, D. H. *Atlas of Zeolite Structure Types*; Butterworth-Heinemann: London, 1992.

(35) Spek, A. L. *Acta Crystallogr.* **1990**, *A46*, C34.

(36) Harrison, W. T. A.; Hanooman, L. *Angew. Chem., Int. Ed. Engl.* **1997**, *36*, 640.

(37) Morimoto, C. N.; Lingafelter, E. C. *Acta Crystallogr.* **1970**, *B26*, 335.

(38) Giacotti, V.; Giordino, F.; Randaccio, L.; Ripamonti, A. *J. Chem. Soc. A*, **1968**, 757.

(39) Harrison, W. T. A.; Nenoff, T. M.; Gier, T. E.; Stucky, G. D. *Inorg. Chem.* **1993**, *32*, 2437.